Title: Increasing growth rate slows adaptation when genotypes compete for diffusing resources

Author names and affiliations

Jeremy M. Chacón
University of Minnesota
Department of Ecology, Evolution, and Behavior
Biotechnology Institute
1479 Gortner Ave., St. Paul, MN 55108
Chaco001@umn.edu

William R. Harcombe **(corresponding author)**
University of Minnesota
Department of Ecology, Evolution, and Behavior
Biotechnology Institute
1479 Gortner Ave., St. Paul, MN 55108
harcombe@umn.edu

Abstract

The rate at which a species responds to natural selection is a central predictor of the species' ability to adapt to environmental change. It is well-known that spatially-structured environments slow the rate of adaptation due to increased intra-genotype competition. Here, we show that this effect magnifies over time as a species becomes better adapted and grows faster. Using a reaction-diffusion model, we demonstrate that growth rates are inextricably coupled with effective spatial scales, such that higher growth rates cause more localized competition. This has two effects: selection requires more generations for beneficial mutations to fix, and spatially-caused genetic drift increases. Together, these effects diminish the value of additional growth rate mutations in structured environments.

Introduction

Species can adapt to environmental change through the fixation of beneficial alleles. If the rate of fixation is too low, species may face consequences such as extinction in changing environments (Campos & Wahl, 2010; Durrett & Levin, 1998). Life in a spatially-structured habit is generally thought to slow the rate of adaptation (Claudino, Lyra, Gleria, & Campos, 2013; Gordo & Campos, 2006; Habets, Czárán, Hoekstra, & De Visser, 2007; Perfeito, Pereira, Campos, & Gordo, 2008). This is because in spatially-structured environments, competitive interactions are more likely to be localized, and so individuals with a beneficial mutation more often compete with themselves than with ancestors (Habets et al., 2007). However, localized interactions are not a requirement of spatial structure (Chacón, Möbius, & Harcombe, 2018): slow resource acquisition rates can result in population dynamics which resemble a well-mixed system. Therefore, it is uncertain

whether the effect of spatial structure on the rate of adaptation is constant or dependent on the biological and environmental details of the species examined.

The relationship between spatial structure and the rate of adaptation is not clear. Sometimes, a rare genotype can benefit from spatial structure, for example when an allelopathic genotype is surrounded by susceptible competitors (Durrett & Levin, 1997; Greig & Travisano, 2008). However, this benefit of structure can become a detriment if reduction in founder density puts allelopaths too far from susceptible targets or too close to cheaters (Gerardin, Springer, & Kishony, 2016; Greig & Travisano, 2008). When spatial structure sufficiently localizes interactions, it can compound other mechanisms which affect the rate of adaptation. For example, epistatic interactions between mutations can result in reduced rates of adaptation that diminish the effect of additional mutations (Chou, Chiu, Delaney, Segre, & Marx, 2011; De Visser, Zeyl, Gerrish, Blanchard, & Lenski, 1999; Khan, Dinh, Schneider, Lenski, & Cooper, 2011; Maddamsetti, Lenski, & Barrick, 2015), and these diminishing returns can be compounded by spatial structure (Campos & Wahl, 2010). Similarly, spatial structure can increase genetic drift and founder effects, thereby reducing the rate of adaptation (Chacón, Möbius, & Harcombe, 2018; Korolev, Xavier, Nelson, & Foster, 2011). However, neither of these negative effects of spatial structure on the rate of adaptation are universal: they can be ameliorated by increased dispersal rates or resource diffusion, which serve to make a system more well-mixed (Gonçalves, De Oliveira, Rosas, & Campos, 2007; Habets et al., 2007; Weinstein, Lavrentovich, Möbius, Murray, & Nelson, 2017). Therefore, to predict the evolution of species in spatially-structured environments, it is imperative to quantitatively understand when, how, and why spatial structure localizes interactions, and the causal consequences of such localization on the rate of adaptation. Here we test how growth rate affects the influence of spatial structure on the rate of adaptation. We hypothesized that, due to the localizing effect that high resource uptake has on competitive interactions (Chacón, Möbius, & Harcombe, 2018), higher basal growth rates will require more generations for beneficial mutations to fix.

Results

We tested the rate at which beneficial mutations increase in frequency in well-mixed and spatially-structured environments. In spatial environments, we conducted simulations in which founder cells were randomly arranged on a toroidal lattice. Five percent of founders were mutants that grew 10% faster than the ancestor. Resources were initially homogeneously distributed, and spread via diffusion as they were consumed. Simulations ran until 99% of the resources were consumed. Then, we applied a bottleneck to the population, selecting new founder cells proportional to final biomass to seed a fresh environment with new random locations (Fig. 1A). Our main independent variable was the absolute growth rate of the population. We tracked the mutant frequency over each transfer (Supp Fig. 1A). Liquid simulations were equivalent to spatial simulations, except there was no spatial structure. We found that in liquid culture, the invasion rate of the mutant was independent of the ancestor's growth rate (Fig. 1B), consistent with invasion rate being set by relative growth rate rather than absolute growth rate. In contrast, in spatial simulations, the mutant invasion rate decreased with the ancestor's growth rate.

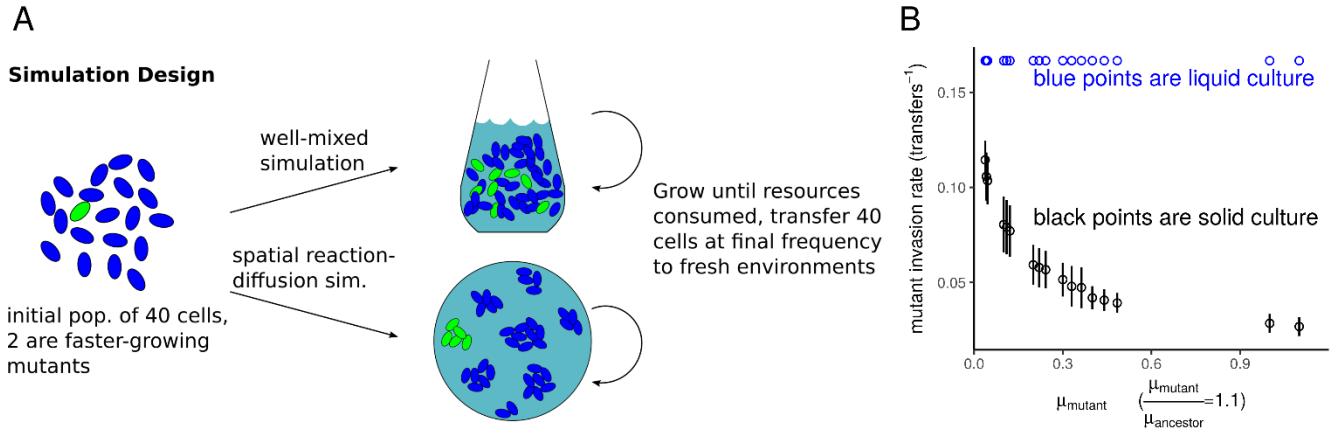

Figure 1: The invasion rate of beneficial mutants in a spatially-structured environment is slower when the absolute growth rate is larger. A) Schematic for the simulation experiment using resource-explicit models with Monod growth. Founder populations of ancestors and faster-growing mutants (at 5% frequency) were seeded into well-mixed or spatially-explicit environments. Different ancestor growth rates were tested, and the mutants always had the same relative growth rate benefit. A simulation continued until 99% of resources were consumed, then a new founder population was seeded into a fresh environment at the frequency observed at the end of the previous simulation. Transfers continued until the mutant reached 90% frequency. The mutation invasion rate was calculated as the inverse of the number of transfers until this threshold was reached. B) The mean mutant invasion rate as a function of the absolute growth rate, for well-mixed (liquid, blue) and spatially-explicit (solid, black) simulations. Error bars are standard error over fifteen replicates. See supplemental FIgure 1A for the time-series from which these data were taken.

Why did the rate of adaptation in the structured habitat decrease as absolute growth rates increased? The rate of adaptation is slower in spatially-structured habitats than in well-mixed habitats (Claudino et al., 2013; Gordo & Campos, 2006; Habets et al., 2007; Perfeito et al., 2008). However, this does not explain the increasing difference in rates. Spatial structure, or more specifically the degree of localization of competitive interactions, is not a binary variable. It changes depending on resource diffusivity (Allison, 2005; Menon & Korolev, 2015; Stump, Johnson, & Klausmeier, 2018) and the proximity and growth rate of individuals (Chacón et al., 2018). Therefore, we sought to quantify spatial structure, specifically by quantifying the degree to which interactions were localized.

We scaled our reaction-diffusion model towards this end, and found that three variables could be combined into a single variable. The scaling procedure (see Materials and Methods) showed that

$$\hat{x} = \frac{x}{\sqrt{D/\mu}}$$

Here, $\hat{x}$ is the scaled distance parameter, x is the unscaled distance variable, D is the diffusion constant of the resource, and μ is the organism's growth or uptake rate. A similar natural length scale was recently observed in a Lotka-Volterra model (Vallespir Lowery & Ursell, 2018), but its relevance to adaptation has not been explored. Does increasing $\hat{x}$ increase the amount of structured interactions? We ran simulations with varying levels of $\hat{x}$, and measured the "territory response" (aka "Voronoi response"), a metric we previously showed scales with the localization of competitive interactions Increasing $\hat{x}$ increased territory response, thereby increasing the effect of spatial structure, until a plateau (Figure 2). By our scaling, increases in $\hat{x}$ are equivalent to increases in growth rate while the distances between founders, and resource

diffusion, are held constant. Therefore, the diminishing returns of adaptation as growth rate increases (Figure 1) are caused by an increase in the effect of spatial structure, due to growth rate's causal effect on local structuring of interactions.

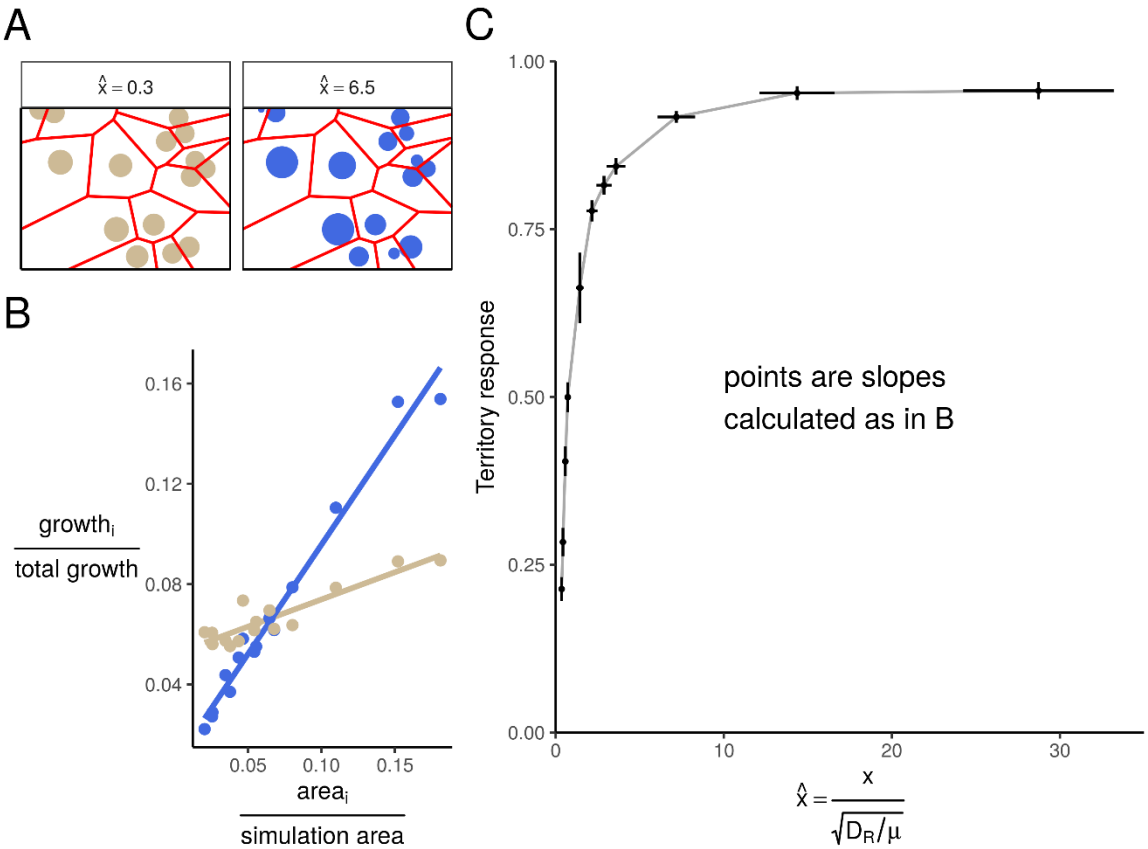

Figure 2. Local structuring of interactions is determined by $\hat{x}$. Scaling the resource-explicit spatial Monod model collapsed three parameters, x (distance), D_R, (resource diffusion constant), and μ (maximum growth rate) into a single variable, $\hat{x} = x/\sqrt{D_R/\mu}$. Simulations using different values of $\hat{x}$ result in different amount of variability in colony size, which also depends on the geometry (founder cell locations) of the simulation. A) Circles represent growth of colonies begun with a single founder cell in a spatial environment after resources have been exhausted. Circle size is proportional to the relative growth (growth of the focal colony / total ecosystem productivity). Note that the low $\hat{x}$ simulation resulted in colonies with more uniform growth yields than the simulation with the higher $\hat{x}$. The lines designate the Voronoi polygons, or "territories". Each polygon encloses the territory closer to the enclosed colony than to any other colony. B) A plot of relative growth over relative territory size for the two simulations shown in A. Note that the simulation with higher $\hat{x}$, which had more variable colony size, has a higher slope. The value of this slope, determined by linear regression, we call the "territory response." C) A plot of territory response over $\hat{x}$ for 15 different simulations (geometries) per $\hat{x}$. Vertical error bars are standard error of territory response. Horizontal error bars are standard error of $\hat{x}$. $\hat{x}$ was variable because different geometries cause the colonies to have different mean distances to nearest neighbors. $\hat{x}$ in C) was calculated by mean nearest neighbor distance in lattice units * width of a lattice unit (in cm) / $\sqrt{D_R/\mu}$. In other words, a simulation with 15 founders that began clustered would have a smaller $\hat{x}$ than simulations with 15 founder cells arranged in the same lattice in a grid at the maximum possible inter-colony distance.

Increasing growth rate increased the local structuring of interactions (Fig. 2) and decreased the rate of adaptation (Fig. 1). We next tested why increasing the local structuring of interactions decreases the rate of adaptation. Local structuring of interactions can cause genetic drift (Korolev et al., 2011). Therefore, we examined the rate of genetic drift among a set of neutral genotypes as a function of $\hat{x}$. We ran spatial simulations with neutral genotypes randomly seeded on a toroidal

lattice, and measured the variation in the change in frequency after resources were consumed (Fig. 3A). Since the genotypes all had the same growth rate, any variation in frequency is purely due stochastic effects of initial locations. We found that increasing the local structuring of interactions, by increasing $\hat{x}$, increased genetic drift (Fig. 3B).

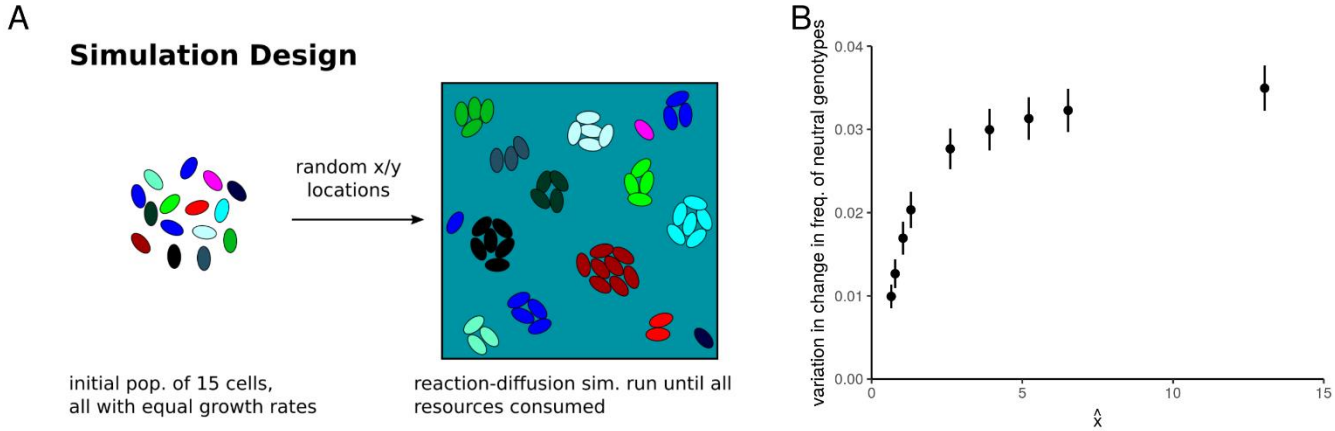

Figure 3. Increasing the local structuring of interactions increases genetic drift. A) Experimental design for the simulations. Fifteen founder cells with equivalent growth characteristics but different neutral genotypes (indicated by color) were seeded into a toroidal spatial environment. These cells were allowed to grow into colonies until 99% of the resources were consumed. The change in frequency (final frequency – 1/15) was measured for each genotype, and the standard deviation of these changes was calculated. Fourteen replicate simulations with different founder locations were ran per $\hat{x}$. B) The variation in the change in frequency of the neutral genotypes, as a function of $\hat{x}$. The points are means of the standard deviation of the change in frequency, averaged across replicates, and the error bars are standard error of this mean.

Finally, we examined how the local structuring of interactions might affect the rate of selection in an environment without genetic drift. We setup simulations in which founder cells were arranged in a grid with equal inter-colony spacing which removed the stochastic effects of territory size. The 'center' cell was a mutant with a 10% growth rate advantage (Fig. 4A). We ran simulations along a gradient of $\hat{x}$, and measured the change in frequency of the mutant after resources were exhausted. The mutant had a smaller increase in frequency, and therefore was selected for less strongly, when $\hat{x}$ was larger (Fig. 4B). Simulations combining random founder locations with non-neutral genotypes show that increasing genetic drift and decreasing selection co-occur with higher local structuring of interactions (Supp. Fig 2).

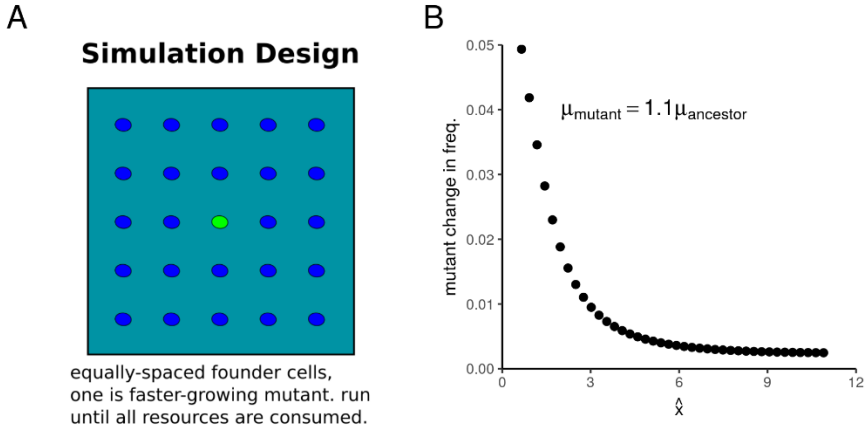

Figure 4: Selection decreases with local structuring of interactions. A) Simulation Design: founder cells were initialized on a toroidal lattice with equal inter-colony spacing. The "center" colony was always a beneficial mutant genotype with a 10% growth rate advantage. Simulations were performed along a gradient of $\hat{x}$ and ran until

resources were consumed, at which point the change in frequency of the beneficial mutant was measured. B) The change in frequency of the mutant genotype as a function of $\hat{x}$.

Discussion

We showed that increased local structuring of interactions reduces the rate of adaptation and increases the rate of genetic drift in spatial environments where resources diffuse. Increases in growth rate increase the local structuring of interactions. Therefore, series of beneficial mutations will progressively decrease the rate of adaptation and increase the rate of genetic drift.

Decreasing rates of adaptation to a specific environment are commonly observed (e.g. Wiser et al 2013). The bio-physical cause of diminishing returns shown here is distinct from the diminishing returns due to genetic effects described in well-mixed populations. In well-mixed populations, adaptation can slow because epistatic interactions reduce the benefit of secondary mutations (Chou et al., 2011; Khan et al., 2011; Kryazhimskiy, Rice, Jerison, & Desai, 2014). Here, we showed that diminishing returns result from the fact that increases in growth rate serve to strengthen the effect of spatial structure. High growth rates make it more likely a founder population competes only with neighbors, which decreases the proportion of environment-wide resources the founder consumes, and therefore decreases the founder's change in allele frequency. In well-mixed populations only relative growth rates matter, while in structured environments absolute growth rates also play a critical role in determining the fate of alleles.

Higher ancestral growth rates reduce selection and are therefore likely to influence evolution of other phenomena. Toxin producers generally gain an advantage from high density because they get more of a return for killing competitors (Greig & Travisano, 2008). Interestingly, the optimal toxin production rate is predicted to decrease with increases in density because too much production increases the chance that cheaters reap the returns from killed competitors (Gerardin et al., 2016). Our results suggest that this relationship will change depending on absolute growth rates, because higher growth rates tend to counteract the effects of higher density. Relatedly, since high growth rates are more likely to restrict interactions to neighbors, we would expect that fast-growing cooperator species are more easily able to exclude cheaters (Borenstein, Meir, Shaevitz, & Wingreen, 2013). Finally, since the selective benefit of growth-rate increases declines in spatial structure, other beneficial phenotypes such as movement or toxicity may be more likely to increase in fitness when the background population has a high growth rate.

Considered broadly, our results suggest that absolute growth rate alters the evolutionary trajectory of sessile organisms that compete for diffusing resources. While we modeled bacteria in a homogenous environment we expect a similar effect in scenarios such as when plants compete for nutrients or water in the soil. Higher growth rates will generally reduce the local pool of resources, thereby reducing selection and increasing drift. The inextricable relationship between growth rate, density and localization of interactions alters fundamental properties of evolutionary trajectories.

Materials and Methods

All of the simulations used a reaction-diffusion partial-differential equations model. Bacteria (B) grew based upon their maximum growth rate (μ), the local resource concentration (R), and Monod kinetics with a half-saturation constant (k). As bacteria grew, resources were consumed with an efficiency parameter (λ). Both bacteria and resources spread via diffusion, with separate diffusion constants (D). We usually simulate two different bacterial genotypes (B_i), which in the fully-parameterized model each have their own maximum growth rates. The following three equations are the "full" model:

$$\frac{\partial B_1}{\partial t} = diffusion + growth = D_{B1}\frac{\partial^2 B_1}{\partial x^2} + B_1\mu_1\frac{R}{R+k_1}$$

$$\frac{\partial B_2}{\partial t} = D_{B2}\frac{\partial^2 B_2}{\partial x^2} + B_2\mu_2\frac{R}{R+k_2}$$

$$\frac{\partial R}{\partial t} = D_R\frac{\partial^2 R}{\partial x^2} - \lambda_1 B_1\mu_1\frac{R}{R+k_1} - \lambda_2 B_2\mu_2\frac{R}{R+k_2}$$

We rescaled this model. First, we made state variables dimensionless by division with characteristic quantities of the same dimension:

$$\hat{R} = \frac{R}{R_c}, \widehat{N_1} = \frac{N_1}{N_c}, \widehat{N_2} = \frac{N_2}{N_c}, \hat{t} = \frac{t}{t_c}, \hat{x} = \frac{x}{x_c}$$

We also redefine the growth rates, resource efficiencies, and Monod constants of bacterial species beyond the first based on their proportion relative to the first species:

$$\lambda_2 = \lambda_1\lambda_c, \mu_2 = \mu_1\mu_c, k_2 = k_1 k_c$$

We also set the species diffusion constants equal to each other, and make them proportional to the resource diffusion constant:

$$D_{B1} = D_{B2} = D_R D_c$$

And finally we define the following characteristic variables:

$$t_c = \frac{1}{\mu_1}, x_c = \sqrt{t_c D_R} = \sqrt{\frac{D_R}{\mu_1}}, R_c = k_1, N_c = \frac{k_1}{\lambda_1}$$

With the chain rule and some algebra this simplifies the reaction-diffusion model into the following set of equations, which we refer to as the "scaled" model (hats are omitted for clarity):

$$\frac{\partial B_1}{\partial t} = D_c\frac{\partial^2 B_1}{\partial x^2} + B_1\frac{R}{R+1}$$

$$\frac{\partial B_2}{\partial t} = D_c\frac{\partial^2 B_2}{\partial x^2} + B_2\mu_c\frac{R}{R+1}$$

$$\frac{\partial R}{\partial t} = \frac{\partial^2 R}{\partial x^2} - B_1\frac{R}{R+1} - \lambda_c B_2\mu_c\frac{R}{R+k_c}$$

The most interesting result of this scaling, discussed in the Results, is that the variable representing space ($\hat{x}$) is a function of 'real' space (x) as well as bacterial growth rates and resource diffusion:

$$\hat{x} = \frac{x}{\sqrt{D_R/\mu_1}}$$

The simulations shown in Figure 1 used the full model (although in practice one can go between the full and scaled model after the fact by using the algebraic conversion). For these simulations, a toroidal world with 3.2 cm per "side" was simulated, discretized into 64 x 64 boxes (i.e. 0.05cm / box). D_R = 5e-6 cm^2 / s, which is typical for a small sugar in water or a 1% agar Petri dish (Chacón et al., 2018). D_{B1} = D_{B2} = 5e-9 cm^2 / s, i.e. 1000x smaller than the constant for the resource. k1 = k2 = 1, meaning when there was one cell equivalent of resource left, the growth rate was at half-maximum. $\lambda_1 = \lambda_2 = 1$. Initially, the entire environment contained 409600 resources, i.e. 100 / box. μ_2 was specified in the figure (as μ_{mutant}) and was always = $1.1\mu_1$. Bacteria were seeded at 40 randomized locations with a value of 1 each. 5% of these were the faster-growing mutant cells. With these boundary conditions, the simulation was ran until 99% of all resources were consumed. Once this threshold was reached, the frequency of the faster-growing mutant was calculated. A new environment was generated with new founder locations, and the starting frequency of the bacteria was, allowing for rounding, equal to the final frequency from the previous simulation. These batch-transfer simulations continued until the mutant reached 90% frequency. Eight replicate batch-transfer experiments were simulated per growth rate, with different founder bacterial locations in each replicate. We also performed equivalent simulations (same founder densities, resource concentrations, growth rates) in mass-action liquid environments.

Simulations testing the relationship between $\hat{x}$ and the Voronoi response (Figure 2) used the scaled model. Each simulation environment used a lattice with 101 x 101 boxes. These simulations used a square (rather than toroidal) lattice, to simplify measurements of the Voronoi response. Bacteria were seeded in 15 random locations with 1 cell / box. To track the growth from each founder cell, each founder had its own differential equation. The diffusion constant of the bacteria was 1/1000 that of the resource. The initial resource concentration was 100 cell-equivalents per box. Simulations were run until 99.999% of the resources were consumed, i.e. the bacteria in all simulations went through the same number of generations. Fifteen replicates were simulated per $\hat{x}$ value. Each replicate had unique founder locations, which were the same for each $\hat{x}$. Once simulations were complete, the Voronoi response was calculated. This was done by measuring the Voronoi area for each founder cell using the dirichletAreas function of the spatstat package in R. Voronoi areas were scaled into relative Voronoi areas by dividing each area by the total simulation area. Relative yields were calculated by dividing the total growth from each founder cell by the total productivity of the simulation. The Voronoi response was then calculated by finding the slope of the linear regression of the relative yields over the relative Voronoi areas (Fig. 2B).

Simulations testing the relationship between $\hat{x}$ and the rate of genetic drift (specifically, variance in change in frequency of neutral alleles, Fig. 3) used the same simulation results as the simulations testing the relationship between $\hat{x}$ and the Voronoi response. There were 15 different simulations per $\hat{x}$.

Simulations examining the influence of $\hat{x}$ on selection when drift cannot (Fig. 4) used the scaled model, again with a toroidal lattice of 65 x 65 boxes, each holding 100 resources. 25 founder cells were placed at equidistant locations in a grid. One founder had a 10% growth rate

advantage. Simulations were ran until 99% of the resources were consumed, and the increase in frequency of the growth-rate mutant was measured.

The simulations in Supp. Fig. 2 examining the influence of $\hat{x}$ on both drift and selection used the scaled model, again with a toroidal lattice of 101 x 101 boxes, each holding 100 resources. Fifteen bacterial cells were placed at random locations. Each cell had a different non-neutral genotype, corresponding to a maximum growth rate. These growth rates were equally spaced from 0.1 to 1.1 along the 15 genotypes. Simulations were ran until 99% of the resources were consumed. Then, a bottleneck was applied which determined which genotypes would survive to become one of the fifteen new cells founding the next season. The founder cells were chosen proportional to the genotypes' relative growth. In addition to the spatial simulations, a corresponding well-mixed simulation was ran, which contained the entire 101x101x100 resources spread in the spatial simulations. The same bottleneck was imposed to the well-mixed simulation. Finally, the genotypes which survived the bottleneck in the spatial simulations were compared to the genotypes which survived the bottleneck in the well-mixed simulations. The response variables plotted in Supp. Fig. 2 are the slow growing genotypes which survived the bottleneck in the spatial simulation but not in the well-mixed simulation, as well as the fast-growing genotypes which persisted in the well-mixed simulation but not in the spatial simulations. Both of these responses are examples where spatial-structure-driven genetic drift overpowered the growth rate selection.

All simulations were coded and ran in R. While we initially planned on using the ReacTran package to numerically solve each reaction-diffusion simulation, we found that we could run the simulations much faster and with fewer errors if we iteratively performed each growth step (done per-box using deSolve's ode function) and diffusion step (using all boxes). Diffusion calculations used a simple forward finite differences scheme, and therefore the time step was kept <= $0.1 * dx^2 / D$, where dx was the width of a box and D was the maximum diffusion constant. This ensured accuracy of the diffusion results. R simulations were run using the University of Minnesota's Minnesota Supercomputing Institute. Code to run example simulations are provided in Supplementary files 1.

Acknowledgements

We thank Mike Travisano and members of the Harcombe lab for useful feedback on this manuscript. Funding for this work was provided by the NIH as project #1R01GM121498-01A1 to William R. Harcombe.

Competing Interests

The authors have no competing interests.

References

Allison, S. D. (2005). Cheaters, diffusion and nutrients constrain decomposition by microbial enzymes in spatially structured environments. *Ecology Letters*, *8*(6), 626–635. http://doi.org/10.1111/j.1461-0248.2005.00756.x

Borenstein, D. B., Meir, Y., Shaevitz, J. W., & Wingreen, N. S. (2013). Non-Local Interaction via Diffusible Resource Prevents Coexistence of Cooperators and Cheaters in a Lattice Model. *PLoS ONE*, *8*(5). http://doi.org/10.1371/journal.pone.0063304

Campos, P. R. A., & Wahl, L. M. (2010). The adaptation rate of asexuals: Deleterious mutations, clonal interference and population bottlenecks. *Evolution*, *64*(7), 1973–1983. http://doi.org/10.1111/j.1558-5646.2010.00981.x

Chacón, J. M., Möbius, W., & Harcombe, W. R. (2018). The spatial and metabolic basis of colony size variation. *ISME Journal*, *12*(3), 669–680. http://doi.org/10.1038/s41396-017-0038-0

Chou, H.-H., Chiu, H.-C., Delaney, N. F., Segre, D., & Marx, C. J. (2011). Diminishing Returns Epistasis Among Beneficial Mutations Decelerates Adaptation. *Science*, *332*(6034), 1190–1192. http://doi.org/10.1126/science.1203799

Claudino, E. S., Lyra, M. L., Gleria, I., & Campos, P. R. A. (2013). Adaptive evolution on a continuous lattice model. *Physical Review E - Statistical, Nonlinear, and Soft Matter Physics*, *87*(3), 1–6. http://doi.org/10.1103/PhysRevE.87.032711

De Visser, J. A. G. M., Zeyl, C. W., Gerrish, P. J., Blanchard, J. L., & Lenski, R. E. (1999). Diminishing returns from mutation supply rate in asexual populations. *Science*, *283*(5400), 404–406. http://doi.org/10.1126/science.283.5400.404

Durrett, R., & Levin, S. (1997). Allelopathy in Spatially Distributed Populations. *Journal of Theoretical Biology*, *185*(2), 165–171. http://doi.org/10.1006/jtbi.1996.0292

Durrett, R., & Levin, S. (1998). Spatial aspects of interspecific competition. *Theoretical Population Biology*, *53*(1), 30–43. http://doi.org/10.1006/tpbi.1997.1338

Gerardin, Y., Springer, M., & Kishony, R. (2016). A competitive trade-off limits the selective advantage of increased antibiotic production. *Nature Microbiology*, *1*(September), 16175. http://doi.org/10.1038/nmicrobiol.2016.175

Gonçalves, E. D. A., De Oliveira, V. M., Rosas, A., & Campos, P. R. A. (2007). Speed of adaptation in structured populations. *European Physical Journal B*, *59*(1), 127–132. http://doi.org/10.1140/epjb/e2007-00260-x

Gordo, I., & Campos, P. R. A. (2006). Adaptive evolution in a spatially structured asexual population. *Genetica*, *127*(1–3), 217–229. http://doi.org/10.1007/s10709-005-4012-9

Greig, D., & Travisano, M. (2008). Density-dependent effects on allelopathic interactions in yeast. *Evolution*, *62*(3), 521–527. http://doi.org/10.1111/j.1558-5646.2007.00292.x

Habets, M. G. J. L., Czárán, T., Hoekstra, R. F., & De Visser, J. A. G. M. (2007). Spatial structure inhibits the rate of invasion of beneficial mutations in asexual populations. *Proceedings of the Royal Society B: Biological Sciences*, *274*(1622), 2139–2143. http://doi.org/10.1098/rspb.2007.0529

Khan, A. I., Dinh, D. M., Schneider, D., Lenski, R. E., & Cooper, T. F. (2011). Negative Epistasis Between Beneficial Mutations in an Evolving Bacterial Population. *Science*, *332*(6034), 1193–1196. http://doi.org/10.1126/science.1203801

Korolev, K. S., Xavier, J. B., Nelson, D. R., & Foster, K. R. (2011). A Quantitative Test of Population Genetics Using Spatiogenetic Patterns in Bacterial Colonies. *The American Naturalist*, *178*(4), 538–552. http://doi.org/10.1086/661897

Kryazhimskiy, S., Rice, D. P., Jerison, E. R., & Desai, M. M. (2014). Global epistasis makes adaptation predictable despite sequence-level stochasticity. *Science*, *344*(6191), 1519–1522. http://doi.org/10.1126/science.1250939

Maddamsetti, R., Lenski, R. E., & Barrick, J. E. (2015). Adaptation, clonal interference, and frequency-dependent interactions in a long-term evolution experiment with escherichia coli. *Genetics*, *200*(2), 619–631. http://doi.org/10.1534/genetics.115.176677

Menon, R., & Korolev, K. S. (2015). Public good diffusion limits microbial mutualism. *Physical Review Letters*, *114*(16), 1–5. http://doi.org/10.1103/PhysRevLett.114.168102

Perfeito, L., Pereira, M. I., Campos, P. R. A., & Gordo, I. (2008). The effect of spatial structure on adaptation in Escherichia coli. *Biology Letters*, *4*(1), 57–59.

http://doi.org/10.1098/rsbl.2007.0481
Stump, S. M. C., Johnson, E. C., & Klausmeier, C. A. (2018). Local interactions and Self-Organized spatial patterns stabilize microbial Cross-Feeding against cheaters. *Journal of the Royal Society Interface*, *15*(140). http://doi.org/10.1098/rsif.2017.0822
Vallespir Lowery, N., & Ursell, T. (2018). Structured environments fundamentally alter dynamics and stability of ecological communities. *Proceedings of the National Academy of Sciences*, *116*(2), 379–388. http://doi.org/10.1073/pnas.1811887116
Weinstein, B. T., Lavrentovich, M. O., Möbius, W., Murray, A. W., & Nelson, D. R. (2017). Genetic Drift and Selection in Many-Allele Range Expansions. *PLoS Computational Biology*, 1–31. http://doi.org/https://doi.org/10.1371/journal.pcbi.1005866